engineering proceedings

MDPI

Proceeding Paper

Frequency Analysis and Transfer Learning Across Different Body Sensor Locations in Parkinson's Disease Detection Using Inertial Signals †

Alejandro Rey-Díaz ‡, Iván Martín-Fernández ‡, Rubén San-Segundo *,‡ and Manuel Gil-Martín *,‡

Grupo de Tecnología del Habla y Aprendizaje Automático (T.H.A.U. Group), Information Processing and Telecommunications Center, E.T.S.I. de Telecomunicación, Universidad Politécnica de Madrid, Madrid, instead. Spain; alejandro.rey.diaz@alumnos.upm.es (A.R.-D.); ivan.martinf@upm.es (I.M.-F.)

* Correspondence: ruben.sansegundo@upm.es (R.S.-S.); manuel.gilmartin@upm.es (M.G.-M.)

† Presented at the 11th International Electronic Conference on Sensors and Applications (ECSA-11), 26–28 November 2024; Available online: https://sciforum.net/event/ecsa-11.

‡ Current address: Av. Complutense 30, 28040, Madrid, Spain.

Abstract: A detailed analysis of the inertial signals input is required when using deep learning models for Parkinson's Disease detection. This work explores the possibility of reducing the input size of the models studying the most appropriate frequency range and determines if it is feasible to evaluate subjects with different sensor locations than those used during training. For experimentation, 3.2-s windows are used to classify signals between Parkinson's patients and control subjects, applying Fast Fourier Transform to the inertial signals and following a Leave-One-Subject-Out Cross-Validation methodology over the PD-BioStampRC21 dataset. It has been observed that the frequency range of 0 to 5 Hz offers a classification accuracy rate of 75.75 ± 0.62% using the five available sensors for training and evaluation, which is close to the model's performance over the entire frequency range, from 0 to 15.625 Hz, which is 77.46 ± 0.60%. Regarding the transfer learning between sensors located in different body parts, it was observed that training and evaluating the model using data from the right forearm resulted in an accuracy of 65.17 ± 0.69%. When the model was trained with data from the opposite forearm, the accuracy was similar, at 63.57 ± 0.69%. Likewise, comparable results were found when using data from the other forearm and when training and evaluating with opposite thighs, with accuracy reductions not exceeding 3%.

Keywords: Parkinson's disease; inertial sensors; convolutional neural networks; fourier transform; PD-BIOSTAMPRC21

Citation: Rey-Díaz, A.; Martín-Fernández, I.; San-Segundo, R.; Gil-Martín, M. Frequency Analysis and Transfer Learning Across Different Body Sensor Locations in Parkinson's Disease Detection Using Inertial Signals. *Eng. Proc.* **2024**, *1*, 0. https://doi.org/

Academic Editor:

Published: 26 November 2024

1. Introduction

Analyzing inertial data offers precise detection on motor anomaly diseases diagnosis, patients monitoring, and evaluation of medical response. Signal processing techniques and artificial intelligence approaches have increased on last years. In particular, their application on healthcare and diseases detection like Parkinson's Disease (PD) becomes really useful for early diagnosis. PD is a neurodegenerative disorder characterized by motor symptoms such as tremor, bradykinesia or rigidity, but affects also to non-motor symptoms including cognitive problems, sleep disorders, and other health problems such as depression or anxiety [1]. Early detection and medical treatment on the first stages of the disease could improve quality of life of the patients, therefore studies on detection with innovative deep learning systems are of great interest [2].

Literature offers a wide number of works focused on human motion modelling [3,4] using deep learning algorithms using wearable sensors, including those focused on PD detection [5–7]. A previous study [8] presented the PD-BioStampRC21 dataset using five inertial sensors over different body locations to detect PD and made a hypothesis stating

that the data received by the thigh sensors provide signals similar to those of the forearms. This aspect was stated because during data collection, the subjects rested their arms on their legs while sitting, so the thigh sensors could extract signals from the arms as well.

Regarding to PD detection accuracy rates using the mentioned dataset obtained in previous works, a previous work [1] obtained a 92.4% accuracy rate using a deep learning architecture and 6.4-s windows of raw data. However, this work used a data distribution that uses signals from the same subject to train and to test the system, simulating an optimistic scenario. Another study [9] used a Leave-One-Subject-Out (LOSO) cross-validation methodology to simulate a more realistic scenario, obtaining a 60.33 ± 1.00% accuracy rate using the same data with 3.2-s windows.

This work proposes the analysis of signal processing techniques and a deep learning neural network in order to identify useful patterns for PD detection and relevant information analyzing different options on the input of the model. Certain experiments have been performed to analyse what information is useful for the model, including the aspect about the hypothesis made by a previous work about the correlation among arms and thighs sensors [8]. In particular, a study of the range of frequencies useful for the detection of the disease has been made. Moreover, this work studies the possibility of training and evaluating the system with sensors in different locations to analyse the transfer learning between them. Then, we first train and evaluate the model with data from a sensor in the same location, and then train the model with a sensor in one location and evaluate it with a sensor in another location, to observe how much the PD detection performance decrease for each sensor pair. Results obtained on these experiments could explain which sensors are suitable for training when another sensor is evaluated particularly. Therefore, the contributions made in this work are:

- Frequency analysis to obtain the frequency range with more useful information for PD detection.
- Transfer learning across the sensor locations on different body parts, discussing accuracy rates acquired training with one sensor and testing with another.

This paper is organized as follows. Section 2 defines the material and methods implemented, including a description of the dataset, the signal processing, the neural network and the evaluation methodology. Section 3 discusses the results obtained by the experimentation and Section 4 exposes the conclusions of this work.

2. Materials and Methods

This section describes the dataset, defines the signal processing techniques, and explains the deep learning neural network and the evaluation methodology used in this work.

2.1. Dataset

The PD-BioStampRC21 dataset [8] comprises tri-axial accelerometer data collected from five wearable sensors, involving both participants with PD patients and healthy controls. The data was gathered using lightweight MC10 BioStamp RC sensors, with each participant wearing five sensors positioned on specific body parts: the chest, left anterior thigh, right anterior thigh, left anterior forearm, and right anterior forearm, as illustrated in Figure 1. The data was sampled at a rate of 31.25 Hz. The dataset features recordings from 34 subjects: 17 healthy controls and 17 PD participants. However, after examining the dataset, it was determined that some sensors from control participants with IDs 007, 014, and 060 had missing data, and thus, those participants were excluded from the study, as done in a previous work [9].

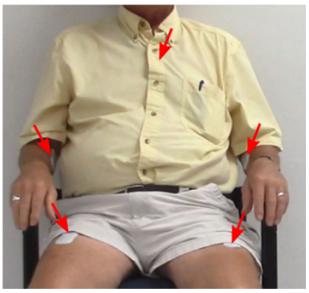

Figure 1. A participant wearing the sensors at five different locations [8].

2.2. Signal Processing

Similar to the baseline system [1], we used 30,000 readings (16.13 min) per participant, along with their health status, to feed the classification system and examine the impact of specific factors.

As observed in a previous work [9], the frequency domain provides more relevant information than the direct raw signals. For this reason, we decided to directly use the Fast Fourier Transform (FFT) coefficients from the inertial signals. Initially, we segmented the recordings into overlapping windows, with a shift equivalent to half the window size between consecutive windows. This way, the system will classify each window as either healthy control or PD based on the participant's health status. We evaluated the classification performance 3.2-s windows, corresponding to 100 time samples, since it was the window length that obtained the best performance over this dataset in a previous work [9].

For obtaining the frequency domain signals, we computed the FFT coefficients for each analysis window, representing the spectrum from 0 Hz to half the sampling frequency, 15.625 Hz for the PD-BioStampRC21 dataset. Since tremor motion energy is primarily concentrated in low frequencies [10], the resulting spectrogram could be beneficial for PD detection.

2.3. Deep Learning Architecture

The deep learning architecture used in this work was a Convolutional Neural Network (CNN), composed of two subnets, as illustrated in Figure 2. First one is the feature learning subnet, which learns features from the input data using convolutional layers with 32 kernels of (1, 5); max-pooling layers with (1, 2) kernel dimensions and ReLU activation function for reducing the impact of gradient vanishing effect. The second one is the classification subnet, applying two dense layers of 64 and 2 dimensions while using on the last layer a SoftMax activation function to offer the predictions of each class for every frame, generating a final classification between PD patient and healthy person. Adam optimizer has been used, setting a learning rate on the neural network, and 30 epochs with a batch size of 100.

Input data dimensions were adapted to each experiment, but they are based on N signals x M samples. N is equivalent to the number of sensors used, being 3 for a single sensor (X, Y and Z signals) and 15 using all five sensors of the dataset. M corresponds to the samples in the frequency domain, which corresponds to 50 samples (half of the 100 samples from the 3.2-s windows). These 50 samples correspond to the frequency range between 0 and 15.625 Hz. M value was different when analyzing frequency ranges. For example, for 0 to 5 Hz, M would be 16, third part of the value of the full range of frequencies.

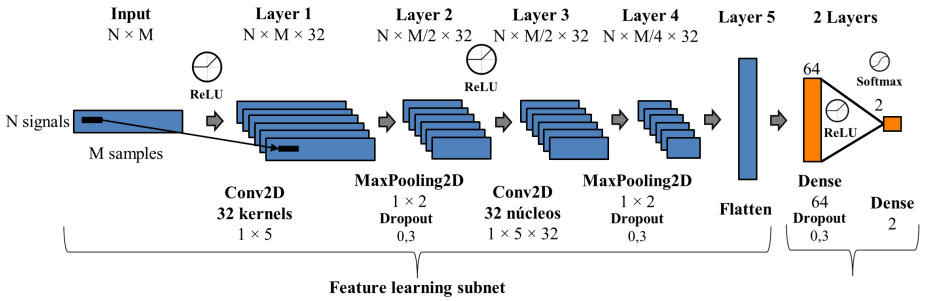

Figure 2. Deep learning neural network used in this work for PD detection.

2.4. Evaluation Methodology

To create a more realistic system, it has been employed a Leave-One-Subject-Out (LOSO) Cross-Validation strategy. This is a specific form of K-fold cross-validation where the system is tested on the data from one subject while being trained on the data from the remaining subjects. This process is repeated multiple times, each time leaving a different subject out for testing, and the final results are averaged across all iterations. This methodology simulates a more challenging and realistic scenario by evaluating the system with recordings from subjects not included in the training data. This creates a realistic system, capable of detecting PD in patients external to the database.

The evaluation metric used in this work is accuracy rate, which is defined in Equation (1), with N testing examples, C classes and P_{ii} being the correct predictions of the model.

$$\text{Accuracy rate} = \frac{1}{N}\sum_{i=1}^{C} P_{ii} \tag{1}$$

In order to represent differences between accuracy rates, confidence intervals (CI) have been used. Only when results surpasses values of other accuracy rates with their confidence interval added, it would represent a real difference. CI are defined in Equation (2), being N the number of testing examples.

$$\text{CI (95\%)} = \pm 1.96 \cdot \sqrt{\frac{\textit{Metric rate} \cdot (100 - \textit{Metric rate})}{N}} \tag{2}$$

3. Results and Discussion

This section describes the experimentation performed in this work, including results and discussion on frequency analysis and transfer learning between different sensor locations.

3.1. Frequency Analysis

As previously mentioned, the sampling frequency of the inertial sensors is 31.25 Hz. This was, the maximum frequency range that could be used to feed the system is between 0 Hz and half of the sampling frequency, 15.625 Hz.

The energy level received from the tremor associated with Parkinson's disease is found at low frequencies, so it is of great interest to find the optimal frequency range for the detection of the disease. Therefore, we studied different frequency ranges to obtain valuable information about Parkinson's tremor: four possible scenarios have been considered for the study.

1. Using the whole available frequency range between 0 and 15.625 Hz.
2. Using the frequency range between 0 Hz and 5.208 Hz.
3. Using the frequency range between 5.208 Hz and 10.417 Hz.
4. Using the frequency range between 10.417 Hz and 15.625 Hz.

As the frequency range decreases in scenarios 2, 3 and 4, the number of samples of the signal is reduced as well, which initially is 50 with all frequencies. By choosing a

frequency range that corresponds to one third of the range used, the number of points will be approximately one third of this value. Table 1 shows the accuracy rates obtained for the different frequency ranges using all the available sensors or each of those separately.

Table 1. Accuracy rates with FFT signals using each sensor as train and test for each frequency range.

Sensor	Frequency Range (Hz)	Accuracy Rate (%)
All	0–15	77.46 ± 0.60
	0–5	75.75 ± 0.62
	5–10	61.87 ± 0.70
	10–15	56.85 ± 0.71
ch—Chest	0–15	73.28 ± 0.64
	0–5	70.34 ± 0.66
	5–10	53.39 ± 0.72
	10–15	46.80 ± 0.72
lh—Left forearm	0–15	65.71 ± 0.68
	0–5	65.95 ± 0.68
	5–10	46.38 ± 0.72
	10–15	44.71 ± 0.72
ll—Left thigh	0–15	62.90 ± 0.69
	0–5	62.15 ± 0.70
	5–10	50.94 ± 0.72
	10–15	48.45 ± 0.72
rh—Right forearm	0–15	64.95 ± 0.69
	0–5	63.68 ± 0.69
	5–10	51.49 ± 0.72
	10–15	48.52 ± 0.72
rl—Right thigh	0–15	64.55 ± 0.69
	0–5	65.77 ± 0.69
	5–10	56.07 ± 0.71
	10–15	43.69 ± 0.71

It can be seen that the accuracy rates from 0 to 5 Hz have very similar values to the whole frequency range for each sensor setup. For example, using all sensors, the system reaches 75.75 ± 0.62% using the first 5 Hz against 77.46 ± 0.60% using the whole frequency range, and using the left thigh sensor, the system reaches 62.15 ± 0.70% using the first 5 Hz against 62.90 ± 0.69% using the whole frequency range . In most sensor setups, there is no significant difference between these two scenarios, such as in the case of the left forearm sensor *lh*, the left thigh sensor *ll*, the right forearm sensor *rh*, and the right thigh sensor *rl*. This way, it could be observed that using the 0 to 5 Hz frequency range and the full frequency range produces similar performance for most independent sensors, decreasing only with the chest sensor *ch* and using all sensors together by maximum value of 3% .

These accuracy rates can be reasoned out due to the nature of the tremor. Figure 3 shows the spectrogram of the right forearm sensor from a PD patient, where we can see that the highest energy level occurs at the 4 Hz frequency. We can also observe high energy levels in the frequencies of its harmonics, at 8 Hz and 12 Hz, but they are lower levels, so the information could really be found in the lower frequency range. The remaining frequencies, being the second and third harmonics, are considered repetitions with lower energy level of the first observable frequency.

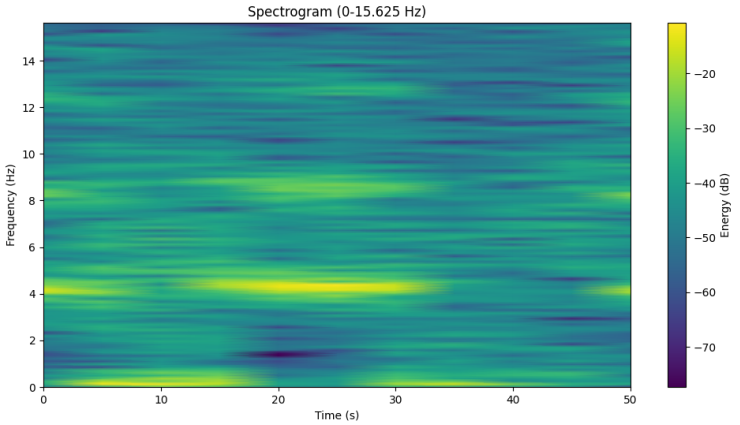

Figure 3. Spectrogram of the signals obtained by the right forearm sensor *rh* from subject with ID 017 of the database.

This result could lead to the possibility of using the third part of the samples in the sensors where the performance is similar, from 0 to 5 Hz, simplifying the input to the model and reducing the training and test time.

3.2. Transfer Learning Across Different Body Sensor Locations

Figure 4 shows the results of the experiments related to training and evaluating the model with sensors in the same or different locations. In the heat map representation, the x axis is related to the sensor used for testing and the y axis is related to the sensor used for training. This way, the principal diagonal shows the results using a specific sensor for training and testing. In addition, the performance values of each column are comparable to each other, since the data used for testing come from the same sensor and location.

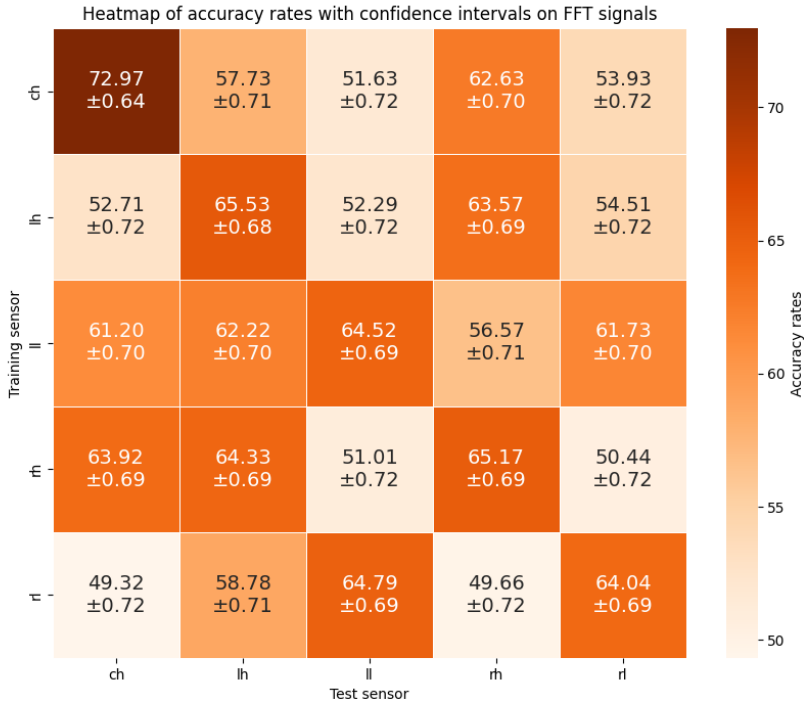

Figure 4. Accuracy rates using different training and testing sensor locations.

In this figure, it can be seen that, naturally, the best rate for each test sensor is obtained when the system is trained with data using the sensor at the same location (results in the principal diagonal). The rest of performance results are related to experiments where we found transfer learning capabilities between sensors, training with a sensor in one location and evaluating with a sensor in another location. In these results, obtaining rates of a similar level means that there exist a tremor relation between those locations.

The results shows how the sensors located in the same location (i.e., arm), but on opposite sides of the body (right or left), offer similar tremor information that allows the possibility of training with one of the sensors, such as the left forearm, and evaluating with the sensor on the opposite side, the sensor on the right forearm, without reducing performance. For example, an accuracy rate of 63.57 ± 0.69% was obtained when training the system with the left forearm and evaluating with the right forearm, compared to the performance of 65.17 ± 0.69%, obtained when training and evaluating with the right forearm sensor. The same behaviour was observed with the thigh sensors.

In addition, it is observed that the hypothesis previously mentioned [8] related to a possible problem with the thigh sensors does not seem to be entirely correct. Analyzing the accuracy rates on both body sides, it can be seen that, for example, training and evaluating with the left thigh *ll* sensor, the system offered an accuracy rate of 64.52 ± 0.69%, and training with the left forearm sensor *lh* and evaluating with the left thigh *ll* sensor, the accuracy rate decreased notably, reaching 52.29 ± 0.72%. This behaviour also occurred for the right thigh and forearm sensors. These results suggest that the thigh tremor was not directly the same as the forearms just because the subjects held their arms over their thighs as the hypothesis of a previous work stated [8].

4. Conclusions

The analysis of the input inertial signals of a deep learning architecture allows the characterisation of useful information from the tremor for PD detection. This work uses 3.2-s windows and a CNN over the PD-BioStampRC21 dataset with five inertial sensors and 31 subjects being PD patients and healthy controls, using a LOSO cross-validation methodology to generate a more realistic scenario.

Analyzing different frequency ranges to feed the system, it has been observed that the first harmonic, located in the range from 0 to 5 Hz, offers a higher performance than the rest of the frequency ranges (5–10 Hz or 10–15 Hz). In addition, in most of isolated sensor setups using the frequency range from 0 to 5 Hz, the model produced accuracy rates without significant difference to those obtained with the whole frequency range. For example using the left thigh sensor, the system reaches 62.15 ± 0.70% using the first 5 Hz against 62.90 ± 0.69% using the whole frequency range from 0 to 15.625 Hz. These results open the possibility of reducing the input size without losing performance.

Regarding the results of transfer learning across different body sensor locations, it can be set that a relationship on a specific sensor and the one in the opposite body part exists. For example, training the model with the left forearm sensor and evaluating with the right forearm, obtains an accuracy rate of 63.57 ± 0.69%, while training and evaluating with the right forearm sensor produces an accuracy rate of 65.17 ± 0.69%. Then, only a 2% reduction of PD detection performance occurred. The same behaviour was observed with the right and left thigh sensors. In addition, evaluating the model with the sensor located on the chest, the right forearm sensor also offers a high accuracy rate.

It is possible to extend this work on future studies. For example, it could be interesting to apply the experimental setups proposed in this work over new datasets with a higher number of subjects in order to certify the results observed in this work. Furthermore, as the results of this work find possible input reduction, and transfer learning across opposite forearms, it could be of great interest developing an interactive wearable application to build real time systems to those who may need those. Moreover, it could be possible to analyse the evolution of the PD disease by creating a regression system to estimate the Unified Parkinson's Disease Rating Scale (UPDRS) from tremor signals.

Author Contributions: Conceptualization, A.R.-D., I.M.-F., R.S.-S. and M.G.-M.; Methodology, A.R.-D., I.M.-F., R.S.-S. and M.G.-M.; Software, A.R.-D. and M.G.-M.; Validation, R.S.-S. and M.G.-M.; Formal analysis, A.R.-D. and M.G.-M.; Investigation, A.R.-D., I.M.-F. and M.G.-M.; Resources, R.S.-S.; Data curation, A.R.-D., I.M.-F. and M.G.-M.; Writing—original draft preparation, A.R.-D. and M.G.-M.; Writing—review and editing, A.R.-D., I.M.-F., R.S.-S. and M.G.-M.; Visualization, A.R.-D. and M.G.-M.; Supervision, R.S.-S.; Project administration, R.S.-S.; Funding acquisition, R.S.-S. All authors have read and agreed to the published version of the manuscript.

Funding: This research received no external funding.

Institutional Review Board Statement: Not applicable.

Informed Consent Statement: Not applicable. Data were collected in another previous work.

Data Availability Statement: The data presented in this study are openly available in IEEE DataPort: https://ieee-dataport.org/open-access/pd-biostamprc21-parkinsons-disease-accelerometry-dataset-five-wearable-sensor-study-0 (accessed on 25 July 2024).

Acknowledgments: This work was funded by Project ASTOUND (101071191—HORIZON-EIC-2021-PATHFINDERCHALLENGES-01) of the European Commission and by the Spanish Ministry of Science and Innovation through the projects TRUSTBOOST (PID2023-150584OB-C21), GOMINOLA (PID2020-118112RB-C22) and BeWord (PID2021-126061OB-C43), funded by MCIN/AEI/10.13039/501100011033 and by the European Union "NextGenerationEU/PRTR". The research of Iván Martín-Fernández was supported by the Universidad Politécnica de Madrid (Programa Propio I+D+i).

Conflicts of Interest: The authors declare no conflicts of interest.

Abbreviations

The following abbreviations are used in this manuscript:

CNN	Convolutional Neural Network
FFT	Fast Fourier Transform
LOSO	Leave-One-Subject-Out
PD	Parkinson's Disease
UPDRS	Unified Parkinson's Disease Rating Scale

References

1. Hathaliya, J.J.; Modi, H.; Gupta, R.; Tanwar, S.; Sharma, P.; Sharma, R. Parkinson and essential tremor classification to identify the patient's risk based on tremor severity. *Comput. Electr. Eng.* **2022**, *101*, 107946. https://doi.org/10.1016/j.compeleceng.2022.107946.
2. Ammenwerth, E.; Nykänen, P.; Rigby, M.; de Keizer, N. Clinical decision support systems: Need for evidence, need for evaluation. *Artif. Intell. Med.* **2013**, *59*, 1–3. https://doi.org/10.1016/j.artmed.2013.05.001.
3. Gil-Martín, M.; López-Iniesta, J.; Fernández-Martínez, F.; San-Segundo, R. Reducing the Impact of Sensor Orientation Variability in Human Activity Recognition Using a Consistent Reference System. *Sensors* **2023**, *23*, 5845. https://doi.org/10.3390/s23135845.
4. Gil-Martín, M.; Johnston, W.; San-Segundo, R.; Caulfield, B. Scoring Performance on the Y-Balance Test Using a Deep Learning Approach. *Sensors* **2021**, *21*, 7110. https://doi.org/10.3390/s21217110.
5. Viteckova, S.; Kutilek, P.; Svoboda, Z.; Krupicka, R.; Kauler, J.; Szabo, Z. Gait symmetry measures: A review of current and prospective methods. *Biomed. Signal Process. Control* **2018**, *42*, 89–100. https://doi.org/10.1016/j.bspc.2018.01.013.
6. San-Segundo, R.; Navarro-Hellín, H.; Torres-Sánchez, R.; Hodgins, J.; De la Torre, F. Increasing Robustness in the Detection of Freezing of Gait in Parkinson's Disease. *Electronics* **2019**, *8*, 119. https://doi.org/10.3390/electronics8020119.
7. San-Segundo, R.; Zhang, A.; Cebulla, A.; Panev, S.; Tabor, G.; Stebbins, K.; Massa, R.E.; Whitford, A.; de la Torre, F.; Hodgins, J. Parkinson's Disease Tremor Detection in the Wild Using Wearable Accelerometers. *Sensors* **2020**, *20*, 5817. https://doi.org/10.3390/s20205817.
8. Adams, J.L.; Dinesh, K.; Snyder, C.W.; Xiong, M.; Tarolli, C.G.; Sharma, S.; Dorsey, E.R.; Sharma, G. A real-world study of wearable sensors in Parkinson's disease. *NPJ Parkinson's Dis.* **2021**, *7*, 106.
9. Gil-Martín, M.; Esteban-Romero, S.; Fernández-Martínez, F.; San-Segundo, R. A Comprehensive Analysis of Parkinson's Disease Detection Through Inertial Signal Processing. In Proceedings of the 16th International Conference on Agents and Artificial Intelligence—Volume 3: ICAART. INSTICC, SciTePress, Rome, Italy, 24–26 February 2024; pp. 462–469. https://doi.org/10.5220/0012360100003636.

10. Gil-Martín, M.; Montero, J.M.; San-Segundo, R. Parkinson's Disease Detection from Drawing Movements Using Convolutional Neural Networks. *Electronics* **2019**, *8*, 907. https://doi.org/10.3390/electronics8080907.